İSTANBUL UNIVERSITY
CERRAHPAŞA

RESEARCH ARTICLE
Electrica 2021; 21(1): 20-31

The Research of Gain Adaptive Linear Extended State Observer (ALESO) Based Active Disturbance Rejection Speed Control For Permanent Magnet Synchronous Motor

Yinsheng Li, Yongjun Chen

Department of Electronic Information, Yangtze University, Jingzhou, Hubei, China

Cite this article as: Li Y, Chen Y. The Research of Gain Adaptive Linear Extended State Observer (ALESO) Based Active Disturbance Rejection Speed Control For Permanent Magnet Synchronous Motor. *Electrica*, 2021; 21(1): 20-31.

ABSTRACT

In this study, linear active disturbance rejection control (LADRC) is used as the speed regulation algorithm of permanent magnet synchronous motor (PMSM) vector control system. It is a fact that the observed gain of traditional linear extended state observer (LESO) is a fixed one and is not able to achieve the dual optimization of noise and disturbance rejection. To solve this optimization problem, this study has proposed the concept of gain adaptive linear extended state observer (ALESO) constructed under gain adaptive regulation law (of ALESO). Then, the proposed mechanism is applied to the speed controller of PMSM vector control system in which the disturbance and noise rejection are evaluated. This study summarizes the parameter characteristics and analyzes the error convergence of ALESO. Finally, the effectiveness of the proposed optimization scheme ALESO is compared with all other existing mechanisms/models for controlling the noise and disturbances and is confirmed by simulation.
Keywords: Vector control of permanent magnet synchronous motor, linear active disturbance rejection control, linear expansion state observer, gain adaptive law

Introduction

A permanent magnet synchronous motor (PMSM) is extensively used in various servo systems because of its high power density, small size and good control accuracy [1–3]. Vector control is the conventional and accepted control mode of PMSM. The traditional PMSM vector control system adopts the double closed-loop mechanism with the current loop as the inner loop and the speed loop as the outer loop. Both the current controller and the speed controller adopt the simple PI control algorithm [4].

Traditional PI control algorithm has the advantages of fixed parameters and simple configuration; moreover, it has the disadvantages of weak anti-interference ability, poor stability, and sensitivity to parameter changes. As PI control algorithm has many limitations, so automatic control experts proposed various optimization schemes, and they have been applied to different control objects [5–8]. Among them, active disturbance rejection control (ADRC), a nonlinear robust control algorithm and improved one of proportional-integral-derivative (PID), does not depend on the specific mathematical model of the controlled object. It treats the parts of the system as lumped disturbances that are unlike the integral standard type, and uses the extended state observer (ESO) to estimate them and introduce equivalent compensation at the control end to suppress the disturbances. In Ref. [9], the nonlinear mechanism of ADRC was simplified and linear adaptive disturbance rejection control (LADRC) was proposed. LADRC has a simple structure constructed based on the complete theoretical analysis [10–12], has few control parameters to be adjusted, and has high engineering application value. Because of its advantages, LADRC has been extensively used in the field of PMSM servo control. In Ref. [13], a PMSM vector control method based on second-order LADRC was proposed. In Refs. [14] and [15], a linear active disturbance rejection speed control scheme for PMSM without position sensor is proposed, which has been applied in practically (actually) in the engineering applications and operations and obtained satisfactory control performance.

Corresponding Author:
Yongjun Chen

E-mail:
yj_ch@163.com

Received: 08.01.2020

Accepted: 23.03.2020

DOI: 10.5152/electrica.2021.20006

However, the linear extended state observer (LESO) of LADRC controller mentioned above uses fixed observation gain and lacks certain disturbance adaptive ability. In Ref. [16], the relationship between the frequency characteristics of LADRC and the parameter configuration is analyzed in frequency domain. This confirms that the observer gain is positively related to the system anti-interference ability, but negatively related to the anti-noise ability. High observation gain can improve the disturbance estimation ability of LESO and aggravate the noise pollution of the system. In Ref. [17], an active disturbance rejection PMSM speed control scheme based on high gain integral (GPI) disturbance observer is proposed, which effectively optimizes the disturbance robustness of the system. However, it does not consider the noise amplification effect of high gain in actual operation. An optimization scheme of anti-noise ability of LESO based on filter is proposed in [18]. The filter is embedded in LESO, which can effectively suppress the measurement noise. However, it will cause certain phase delay and weaken the speediness of LESO. In [19], an adaptive extended state observer (AESO) is proposed and the time-varying law of observation gain is designed. The general idea of ALESO is to adopt a small observation gain at the initial stage to alleviate the peak phenomenon, and then the observation gain gradually increases with time and finally stabilizes at the maximum value. Note that ALESO effectively alleviates the peak effect because of "big error and big gain" in the initial stage, but its observation gain only changes with time, and is fixed at the maximum value in the later stage, thus losing its adaptive ability ultimately. However, similar to Ref. [18], AESO does not consider the suppression of measurement noise.

To effectively reduce the conflict between disturbance robustness and noise suppression performance of LESO, a gain adaptive linear extended state observer (ALESO) is proposed and a gain adaptive regulation law of ALESO is designed in Section 3. Note that, unlike [19], the gain of the ALESO proposed in this study is adaptive to the observed state error rather than time. The gain of ALESO presented in this study has global adaptive capability. The error convergence and parameter adjustment characteristics of ALESO are analyzed in Section 3. Finally, ALESO is applied to LADRC speed controller of PMSM vector control system. In Section 4, the effectiveness of the proposed LADRC speed control method is confirmed by comparing with LADRC speed controller with generalized proportional integral (GPI) observer (GPI-LADRC) [18], LADRC speed controller with high observation gain (HLADRC), and LADRC speed controller with low observation gain (LLADRC) in simulation.

Linear active disturbance rejection speed controller

The control object studied in this study is the surface-mounted permanent magnet synchronous motor (SPMSM). The mathematical model of PMSM is simplified and the current control strategy of i_d=0 is adopted, then the equation of state of PMSM in *d-q* coordinates is as follows

$$\begin{cases} \dot{i}_q = \frac{1}{L_s}\left(-Ri_q - p_n\varphi_f w + u_d\right) \\ \dot{w} = \frac{1}{J}\left(-T_L + \frac{3p_n\varphi_f}{2} i_q - Bw\right) \end{cases} \tag{1}$$

where R and L_S is the stator resistance and the stator inductance, φ_f is the permanent magnetic linkage, i_d and i_q is the axial component of the stator current, J is the moment of inertia, B is the damping coefficient,w is the mechanical angular velocity, T_L is the load torque, and p_n is the polar log.

The vector control system of PMSM is based on equation (1) and Figure 1 is the structure diagram of PMSM vector control system, where ASR is the speed controller and ACR is the current controller. Traditional ASR and ACR adopt simple PI algorithm to track the reference speed w^* and the reference current i_q^*, whose aim is to eliminate errors by the integral and proportional signals of errors.

As shown in Figure 1, load disturbance T_L is the primary disturbance of the system, which is exerted within the speed loop and beyond the current loop. Therefore, to improve the anti-disturbance ability of the speed loop, the speed controller (ASR) can adopt the first-order linear ADRC algorithm; however, the current regulator (ACR) will continue to follow the traditional PI tracking algorithm.

According to Equation (1), the state equation of PMSM vector control speed loop can be obtained as follows:

$$\dot{w} = \frac{3}{2}\frac{p_n\varphi_f}{J} i_q - \frac{B}{J}w - \frac{T_L}{J} \tag{2}$$

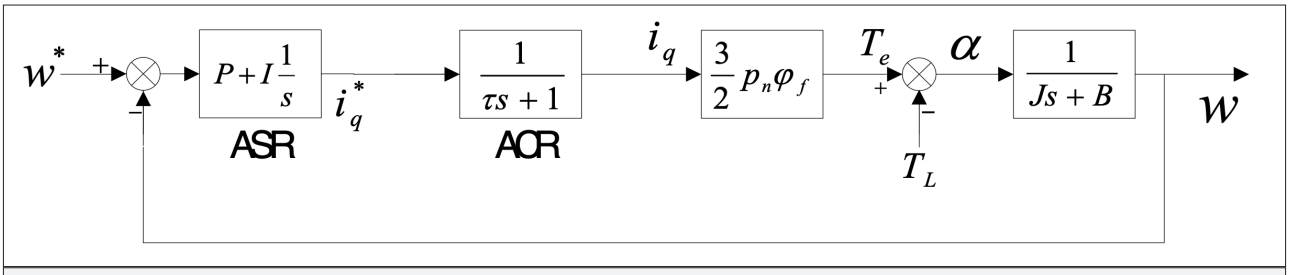

Figure 1. PMSM vector control schematic

Defining u as the control quantity i_q and b as the control gain, that is,

$$b = \frac{3}{2}\frac{p_n \varphi_f}{J}$$

Defining b_0 as the estimated control gain, $(b-b_0)u - \frac{B}{J}w - \frac{T_L}{J}$ is the lumped disturbance f, and the expansion state of the system, then system (2) can be written in a standard form as follows:

$$\begin{cases} \begin{bmatrix} \dot{w} \\ \dot{f} \end{bmatrix} = A_s \begin{bmatrix} w \\ f \end{bmatrix} + B_0 u + \begin{bmatrix} 0 \\ d \end{bmatrix} \\ y = C \begin{bmatrix} w \\ f \end{bmatrix} \end{cases} \tag{3}$$

where $A_s = \begin{bmatrix} 0 & 1 \\ 0 & 0 \end{bmatrix}, B_0 = \begin{bmatrix} b_0 \\ 0 \end{bmatrix}, C = [1 \ \ 0], d$ is the derivative of f.

To reasonably arrange the transition process of the given value, the nonlinear TD is retained. The first-order linear ADRC speed controller can be designed as follows:

The first-order TD:

$$\dot{z}_{11} = -rfal\left(z_{11} - w^*, \alpha_0, \upsilon_0\right) \tag{4}$$

where Z_{11} is the transition process of speed setting, r is the tracking speed factor of TD, $fal(\cdot)$ is nonlinear function as (9), andc α_0 and υ_0 are the nonlinear factor and the width of linear interval of $fal(\cdot)$, respectively.

The observable matrix of (3) is $Q = \begin{bmatrix} C \\ CA \end{bmatrix}$ and

$$rank\, Q = rank \begin{bmatrix} 1 & 0 \\ 0 & 1 \end{bmatrix} = 2$$

So, when d is bounded, system (3) is observed, then linear second-order ESO can be designed for (3) as follows:

$$\begin{cases} \dot{z}_{21} = z_{22} - \beta_{01}\left(z_{21} - w\right) + b_0 u \\ \dot{z}_{22} = -\beta_{02}\left(z_{21} - w\right) \end{cases} \tag{5}$$

where Z_{21} is the tracking value of w, Z_{22} is the estimation value of the comprehensive disturbance f, and [β_{01}, β_{02}] is the state feedback gain matrix of LESO.

Proportional error feedback control law:

$$\begin{cases} u_0 = k_p\left(z_{11} - z_{21}\right) \\ u = u_0 - \frac{z_{22}}{b_0} \end{cases} \tag{6}$$

where k_p is the proportional coefficient of the linear feedback control law and b_0 is the estimated control gain.

Defining $\overline{w}$ as the gain (known as bandwidth) of LESO, according to the "bandwidth parameter setting method" in [9], the equation can be written as follows:

$$\begin{cases} \beta_{01} = 2\overline{w} \\ \beta_{02} = \overline{w}^2 \end{cases} \tag{7}$$

$\overline{w}$ can be either a constant or a variable, and its size determines the disturbance tracking ability of (5).

The state observation error of LESO is $e_1 = z_{21} - w$ and $e_2 = z_{22} - f$. The differential equation of state error of LESO can be obtained by subtracting (3) from equation of state (5) and is as follows

$$\begin{cases} \dot{e}_1 = e_2 - 2\overline{w}e_1 \\ \dot{e}_2 = -\overline{w}^2 e_1 - d \end{cases} \tag{8}$$

is a nonlinear function as given below,

$$fal(x, \alpha, \upsilon) = \begin{cases} x / \delta^{1-\alpha}, |x| \le \upsilon \\ |x|^{\alpha}\, \mathrm{sgn}(x), |x| > \upsilon \end{cases} \tag{9}$$

where α is the nonlinear factor and υ is the width of linear interval.

The principle of LADRC speed control is shown in Figure 2.

Gain adaptive linear extended state observer (ALESO)

3.1 Design of gain adaptive law and analysis of its parameter characteristics

The most essential property of ADRC is disturbance suppression, which uses the extended state observer to estimate and compensate the generalized disturbance of the system. Its main function is separating disturbance rejection control and tracking the control. As the core of LADRC, LESO can be considered as the anti-disturbance controller of LADRC, and its performance plays a decisive role in the anti-disturbance quality of LADRC. The performance of LESO is determined by its observed gain $\overline{w}$. According to the frequency-domain analysis of LADRC and LESO in literature [16], the larger the $\overline{w}$ of LESO, the stronger its tracking ability to disturbance and the better the disturbance robustness of LADRC controller. However, $\overline{w}$ of LESO cannot be infinitely increased because the observation gain of LESO is negatively correlated with its noise suppression ability.

To design a method that achieve the dual optimization of disturbance rejection and noise rejection, this study puts forward the idea of gain adaptive linear extended state observer (ALESO). When the disturbance changes rapidly, a large $\overline{w}$ is used to improve its tracking ability; however, when the disturbance changes slowly, a small $\overline{w}$ is used to reduce the sound (amplification) effect of noise.

However, $\dot{f}$ cannot be directly measured. As the state tracking error $e_1 = z_{21} - w$ is positively correlated with $\dot{f}$. In this study, e_1 replaces $\dot{f}$ as the dependent variable of gain adaptive law

$$\overline{w} = \xi\left(|e_1|\right) \tag{10}$$

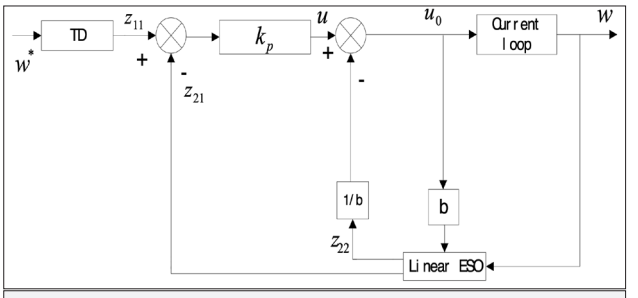

Figure 2. First-order LADRC speed control schematic diagram

Therefore, the state equation of ALESO is as follows:

$$\begin{cases} \dot{z}_{21} = z_{22} - 2\overline{w}(z_{21} - w) + b_0 u \\ \dot{z}_{22} = -\overline{w}^2 (z_{21} - w) \\ \overline{w} = \xi(|e_1|) \end{cases} \tag{11}$$

The gain adaptive law of LESO is proposed as follows:

$$\overline{w} = \xi(|e_1|) = B + a\left(\frac{1}{1+e^{-\mu|e_1|^{\delta}}} - 0.5\right) \tag{12}$$

where $\overline{w}_{\min} = \xi_{\min} = B$, $\overline{w}_{\max} = \xi_{\max} = B + 0.5a$, μ is the sensitivity factor, and δ is the steep factor. The image of the gain adaptive law of (12) is shown in Figure 3.

The gain adaptive law in Figure 3 is divided into five regions: region 1 is the low-gain stationary region, region 2 and 3 are the gain growth regions, and regions 4 and 5 are the high-gain linear regions.

Define v as the measuring noise of the speed of PMSM, when the measurement noise is taken into account, the equation can be written as

$$e_1 = z_{21} - w - v \tag{13}$$

According to (5) and (12), the gain increment relative to the $\overline{w}_{\min}$ is

$$\xi(|e_1|) - B = a\left[\frac{1}{1+e^{-\mu|e_1|^{\delta}}} - 0.5\right] \tag{14}$$

When the complex disturbance f changes slowly,

$z_{21} \approx x_1$, $z_{22} \approx f$

v is the white Gaussian noise, then (14) can be approximated to

$$\overline{w} = \xi(|e_1|) = B + a\left(\frac{1}{1+e^{-\mu|v|^{\delta}}} - 0.5\right) \tag{15}$$

It can be seen that the tracking error in the above case is mainly caused by v, and the gain increment in (14) is mainly affected by the amplitude of v. In this case, the width of the low-gain stationary region should be higher than $2|v|$ to weaken the influence of v on $\overline{w}$ of LESO.

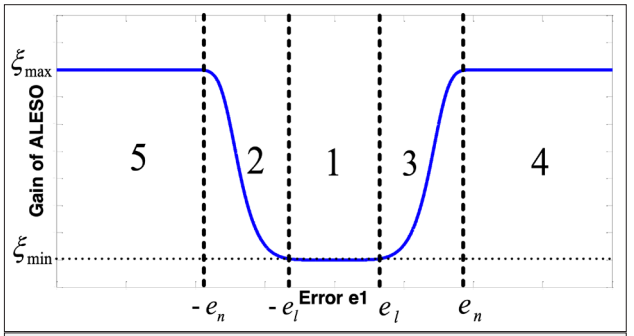

Figure 3. The gain adaptive law $\xi(|e_1|)$

Therefore, the wider the low-gain stationary region is, the less sensitive of $\xi(|e_1|)$ to the tracking error is caused by noise.

The gain growth region is the main area to realize the adaptive adjustment of $\overline{w}$. The steeper it is, the faster $\overline{w}$ responds to the disturbance change.

When $|e_1|$ increases to a certain value, the value of $\overline{w}$ will remain at $\xi_{\max}(|e_1|) = B + 0.5a$ and will not change. At this point, ALESO works in the high-gain linear region. $\xi_{\max}(|e_1|)$ determines the upper limit of the ability of ALESO to estimate the disturbance with large variations, and the existence of high-gain linear region ensures the stability and error convergence of ALESO.

The parametric properties of $\xi(|e_1|)$ are as follows:

The main parameters of gain adaptive regulation law of (12) include α, β, the sensitive factor μ, and steep factor δ.

β and α determine the upper and lower limits of $\overline{w}$ as $\overline{w}_{\max} = \xi_{\max} = B + 0.5a$ and $\overline{w}_{\min} = \xi_{\min} = B$. The larger $\overline{w}_{\max}$ is, the stronger the tracking ability of ALESO is. At the same time, $\overline{w}_{\min}$ determines the filtering effect of ALESO on measurement noise. The smaller $\overline{w}_{\min}$ is, the smaller the gain of ALESO on measurement noise in steady state is, and so a higher tracking accuracy of ALESO in the steady state is achieved.

μ is the sensitive factor of $\xi(|e_1|)$ and its size is negatively correlated with the width of the low-gain stationary region, and positively correlated with the steepness of the gain growth region.

δ is the steepness factor of $\xi(|e_1|)$ and its size is positively correlated with the width of low-gain stationary region and the steepness of gain growth region of $\xi(|e_1|)$.

The gain adaptive principle of ALESO of (11) is as follows: when f changes slowly, the state error $|e_1|$ will be small, and ALESO works in the stable region with low gain and strong noise suppression ability. When the $\dot{f}$ increases, the $|e_1|$ increases. When $|e_1|$ enters the gain growth region, $\overline{w}$ increases rapidly with the increase of $|e_1|$, and the tracking ability of ALESO to f enhances rapidly. When $|e_1|$ continues to increase, ALESO works in the high-gain linear region and the $\overline{w}$ of ALESO remains at the highest value. At this point, the tracking ability of ALESO to f reaches the peak.

Error convergence of gain adaptive linear extended state observer (ALESO)

The following assumption for system (3) and (11) are presumed:

Assumption (a1): The derivative of the f is bounded and satisfies

$$\left\|\dot{f}\right\| \le \gamma \tag{16}$$

Assumption (a2): The $\overline{w}_{\max}$ of ALESO of (11) is satisfied and the equation is as follows

$$\overline{w}_{\max} = \xi_{\max}\left(|e_1|\right) = B + 0.5a > 0 \tag{17}$$

Theorem 1: Suppose that the system (3) of PMSM and the ALESO of (11) satisfies Assumption (a1) and (a2). Then,

The tracking error of ALESO is ultimately bounded and satisfied

$$\|e\| \le \max\left(2\gamma\|P_l\|, \sigma\right) \tag{18}$$

Where *e* is the state tracking error of ALESO and is given by the equation

$$e = \begin{bmatrix} e_1 & e_2 \end{bmatrix}^T = \begin{bmatrix} z_{21} - w & z_{22} - f \end{bmatrix}^T \tag{19}$$

P_1 is the solution of Riccati equation of (20)

$$A_1^T P_1 + P_1 A_1 = -I,\ A_1 = \begin{bmatrix} -2(B+2a) & 1 \\ -(B+2a)^2 & 0 \end{bmatrix} \tag{20}$$

Proof: See Appendix

The simulation verification

SIMULINK graphical programming is used for simulation. The various parameters such as the anti-load capability, parameter robustness and anti-noise capability of LADRC speed controller with 3 orders generalized proportional integral (GPI) observer (GPI-LADRC) [17], LADRC speed controller with high observation gain (HLADRC), LADRC speed controller with low observation gain (LLADRC), and LADRC speed controller with adaptive observation gain (ALADRC) were compared and analyzed with the parameters obtained in simulation. SIMULINK simulation model of PMSM ALADRC speed control system is shown in Figure 16 in Appendix.

The PMSM parameters adopted in the simulation are shown in Table 1. The parameters of the above three kinds of LADRC speed controllers are shown in Table 2 and the parameters of ALADRC are shown in Table 3.

The image of the gain adaptive law of ALADRC for $\xi_{\max}$=4000 and $\xi_{\min}$=500 is shown in Figure 4. The width of the low-gain stationary region is maintained at $|e_1|$≤0.4 to ensure that ALESO has a good suppression effect on noise in a certain range.

The analysis of anti-load capacity

Under no-load condition, the motor speed is accelerated to 1000 from 0 rpm. The load torque suddenly raises to 30 Nm in

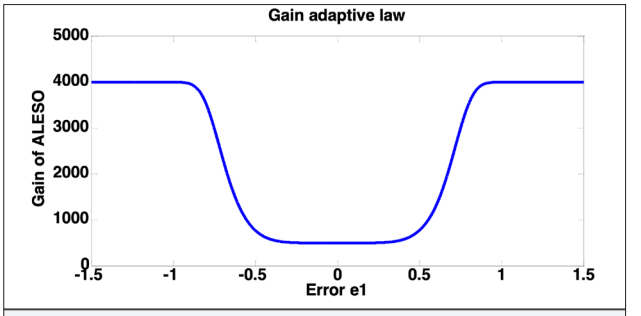

Figure 4. The gain adaptive law of ALESO

Table 1. PMSM parameters of simulation

Parameter	Value	Parameter	Value
R_s/Ω	0.0918	$J/kg\ m^2$	0.003945
L_s/H	0.000975	$B/Ns\ m^{-1}$	0.0004924
φ_f/Vs	0.1688	P	4

In Table 1, R_s is stator resistance of PMSM
L_s is stator inductance of PMSM
φ_f is permanent magnet flux of PMSM
J is moment of inertia of PMSM
B is viscosity of PMSM
P is the polar log of PMSM

Table 2. Parameters of GPI-LADRC, HLADRC, LLADRC speed controller

Parameter	GPI-LADRC	HLADRC	LLADRC
$\overline{w}$	2500	2500	800
k_p	2	2	2
b_0	256.73	256.73	256.73
r	500	500	500
a_0	0.5	0.5	0.5
υ_0	0.01	0.01	0.01

Table 3. Parameters of ALADRC speed controller

Parameter	Value
B	500
a	7000
μ	10
δ	6
k_p	2
b_0	256.73
a_0	0.5
υ_0	0.01

In Tables 2 and 3, $\overline{w}$ is the gain of ALESO
k_p is the proportional coefficient of the linear feedback control law.
b_0 is the estimated control gain.
r is the tracking speed factor of TD
a_0 is the nonlinear factor of $fal(\cdot)$
υ_0 is the width of linear interval of $fal(\cdot)$
B and a determine the upper and lower limits of $\overline{w}$ as $\overline{w}_{max}=\xi_{\max}\left(|e_1|\right)=B+0.5\ a$ and $\overline{w}_{min}=\xi_{\min}\left(|e_1|\right)=B$.
μ and δ is the sensitivity factor and the steep factor of $\xi(|e_1|)$, respectively.

0.2 s, and then, the load torque falls back 0 Nm at 0.25 s. Figure 5 shows the speed response curve of the proposed control method, the HLADRC, the LLADRC, and the GPI-LADRC. The maximum speed fluctuation error, $|e_n|_{\max}$, is shown in Table 4. Figure 6 shows the local amplification of the disturbance estimate $\hat{f}$ of linear extended state observer with low gain (LLESO), linear extended state observer with high gain (HLESO), GPI observer and Gain adaptive linear extended state observer (ALESO). The gain of ALESO is shown in Figure 7.

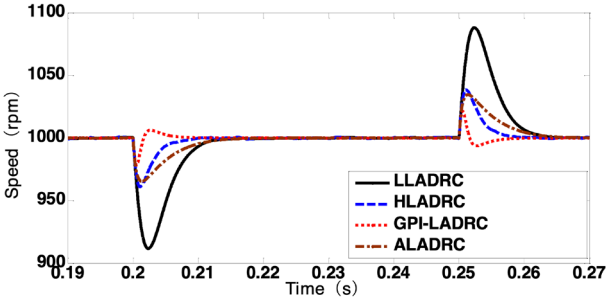

Figure 5. Speed response curve of four control method

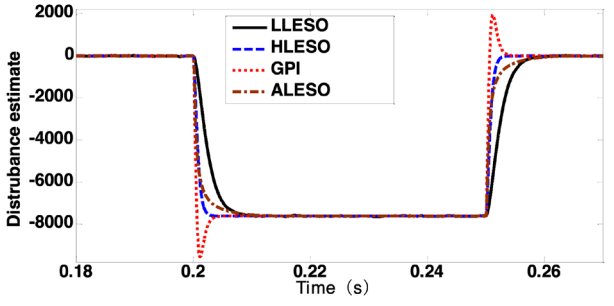

Figure 6. The local amplification of the disturbance estimate $\hat{f}$ of four disturbance observer

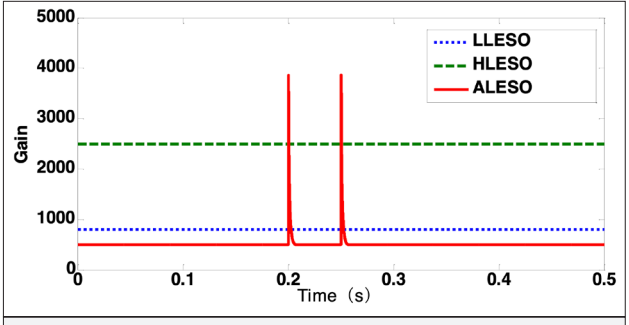

Figure 7. The gain of ALESO

Table 4. The maximum speed fluctuation error $|e_n|_{\max}$ of the four control methods

	$\|e_n\|_{\max}$	
Control method	**Load step up**	**Load step down**
LLADRC	8.83%	8.8%
HLADRC	3.89%	3.8%
GPI-LADRC	2.16%	2.2%
ALADRC	3.46%	3.5%

As can be seen from Figure 5, no matter whether the load steps up or steps down, the rotation speed of three methods fluctuate. The maximum speed fluctuation error of LLADRC is the largest and the recovery time is the longest. The maximum speed fluctuation error of GPI-LADRC was the least, but the speed overshoot occurred about 0.6% during the speed recovery process. The maximum speed fluctuation error of ALADRC is slightly smaller than that of HLADRC, but the speed recovery time is longer than that of HLADRC, and the load resistance capacity of both is similar.

According to Figure 6, it is easy to see that all three disturbance observers can effectively track the f ultimately. Under the same observation bandwidth, GPI observer can track the sudden disturbance caused by load change quickly than HLADRC. However, in the process of disturbance tracking, GPI observer generates a large overshoot estimation error while three other disturbance observers can track f without any overshoot, which is also the reason for the overshoot in the process of speed recovery. LLESO has the slowest tracking speed because of the low gain. The tracking speed for f of ALESO and HLESO is close when the load changes, but the time required for ALESO to reach the steady state is a little longer than HLESO. As can been seen from Figure 7, this is because the gain of ALESO increases rapidly after the sudden change of load, which strengthens the tracking ability of ALESO. When it is close to the steady state, the working state of ALESO returns to the low-gain stationary region, and the disturbance estimate $\hat{f}$ of ALESO finally slowly tends to f.

The analysis of the parameter robustness

The variations of motor parameters will affect the performance of the control system resulting in the deviation of the running point. In order to test the sensitivity of the proposed control method for variable parameters, φ_f is taken as the variable parameter of the motor in this paper. The standard value of φ_f is φ_{fn}=0.1688*Vs*. The PMSM with 20 Nm load runs stably at 1000 rpm, and at 0.2 s, φ_f the steps up from φ_{fn} to $2\varphi_{fn}$. And then at 0.25 s, the φ_f steps down from $2\varphi_{fn}$ to $0.5\varphi_{fn}$. The motor speed response of the four control methods is shown in Figure 8, the estimation of disturbance is shown in Figure 9, the control output i_q^* is shown in Figure 10 and the gain of ALESO is shown in Figure 11.

It can be seen from Figure 8 that the rotation speed of PMSM fluctuates regardless of the φ_f steps up or steps down. The maximum speed fluctuation error, $|e_n|_{\max}$, of the four control methods and the over-regulation of the speed recovery, ε, is shown in Table 5. It can be seen that GPI-LADRC has the min-

imum $|e_n|_{max}$, but the maximum speed over-regulation occurs whether φ_f steps up or load steps down. This is because the GPI observer has a large overestimation in the process of estimating the disturbance, which can be seen from Figure 9. The

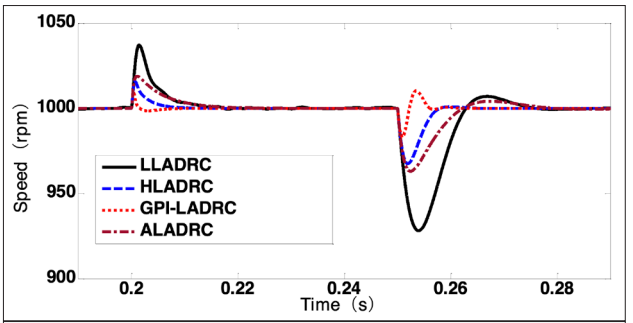

Figure 8. The speed curve of four control method

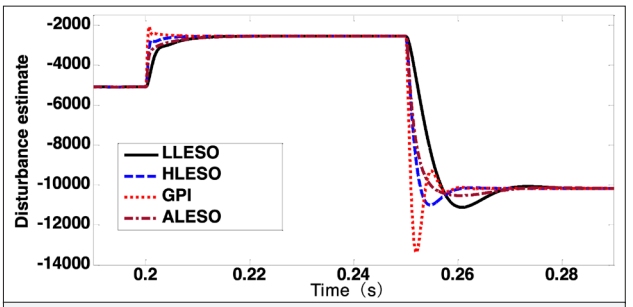

Figure 9. The estimation of disturbance by four observers

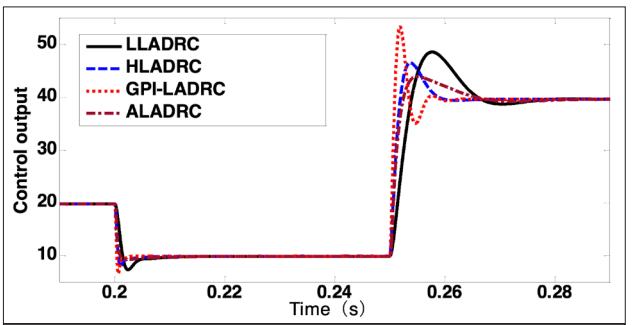

Figure 10. The control output i_q^* of four control method

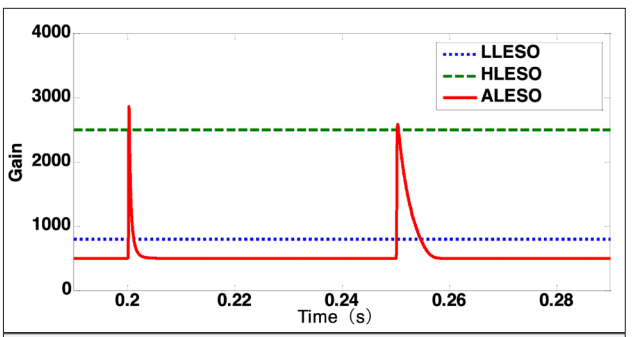

Figure 11. The gain of ALESO

$|e_n|_{max}$ of LLADRC is the largest, and there is a certain speed overshoot in the process of speed recovery after φ_f steps down. The $|e_n|_{max}$ of ALADRC is close to that of HLADRC, but the recovery time of ALADRC is longer. In general, HLADRC has the best robustness and stability for the changes in φ_f.

The estimation of abrupt disturbance by ALESO is effectively buffered by the existence of low gain stationary region, so ALESO has the smallest overestimate of f.

The change of the φ_f is essentially the change of the integrated disturbance of the system, and its principle is consistent with the change of load torque, so the parametric robustness of the system is consistent with the nature of load resistance.

Since i_q^* is directly compensated by $\hat{f}$, the adjustment (change) trend of i_q^* is consistent with that of $\hat{f}$ except in the opposite direction, which can also be obtained by comparing Figure 9 with Figure 10.

Noise suppression performance

In order to track the changing state quantity, LESO adopts a large observation gain that leads to the measure noise amplification and the steady state accuracy of the control system gets affected. In order to verify and compare the noise suppression performance of four speed control methods and the corresponding four disturbance observers, this paper introduces white Gaussian noise with sample time of 0.00005 s and variance of 0.02 at the output of the speed of PMSM to simulate the measurement noise in actual operation. The variation of load torque setting speed is consistent with Section 4.1. The real steady speed control accuracy of four control methods is evaluated by the criterion, that is, by the integral mean of absolute error of speed tracking, IMASE, which is expressed in (30). And the noise suppression performance of the corresponding four disturbance observers is evaluated by the criterion, that is, by the integral mean of absolute error of disturbance estimation, IMADE, which is expressed as in (31)

$$\mathrm{IMASE} = \frac{\int_{t_1}^{t_2} |w^*(t) - w(t)|\,dt}{t_2 - t_1} \tag{30}$$

Table 5. The maximum speed fluctuation error $|e_n|_{max}$ and the over-regulation ε of the four control methods

	φ_f step up		φ_f step down	
Control method	$\|e_n\|_{max}$	**ε**	$\|e_n\|_{max}$	**ε**
LLADRC	3.7%	0	7.18%	0.7%
HLADRC	1.6%	0	3.25%	0.1%
GPI-LADRC	0.9%	0.15%	1.69%	1%
ALADRC	1.9%	0	3.7%	0.4%

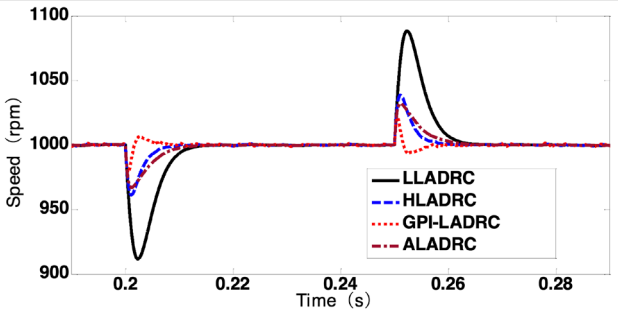

Figure 12. The local amplification of the speed response curve

$$\mathrm{IMADE} = \frac{\int_{t_1}^{t_2} \left| f(t) - \hat{f}(t) \right| dt}{t_2 - t_1} \qquad (31)$$

where (t_1, t_2) is the steady state period of the system.

The local amplification of the speed response curve is shown in Figure 12, and the disturbance estimation $\hat{f}$ of four disturbance observers is shown in Figure 13. Figure 14 shows the control output i_q^* of four speed control methods, and Figure 15 shows the observation gain of ALESO.

Tables 6 and 7, respectively, show the IMADE and IMASE of the four control methods. As seen from Table 7, for either T_L=0 or

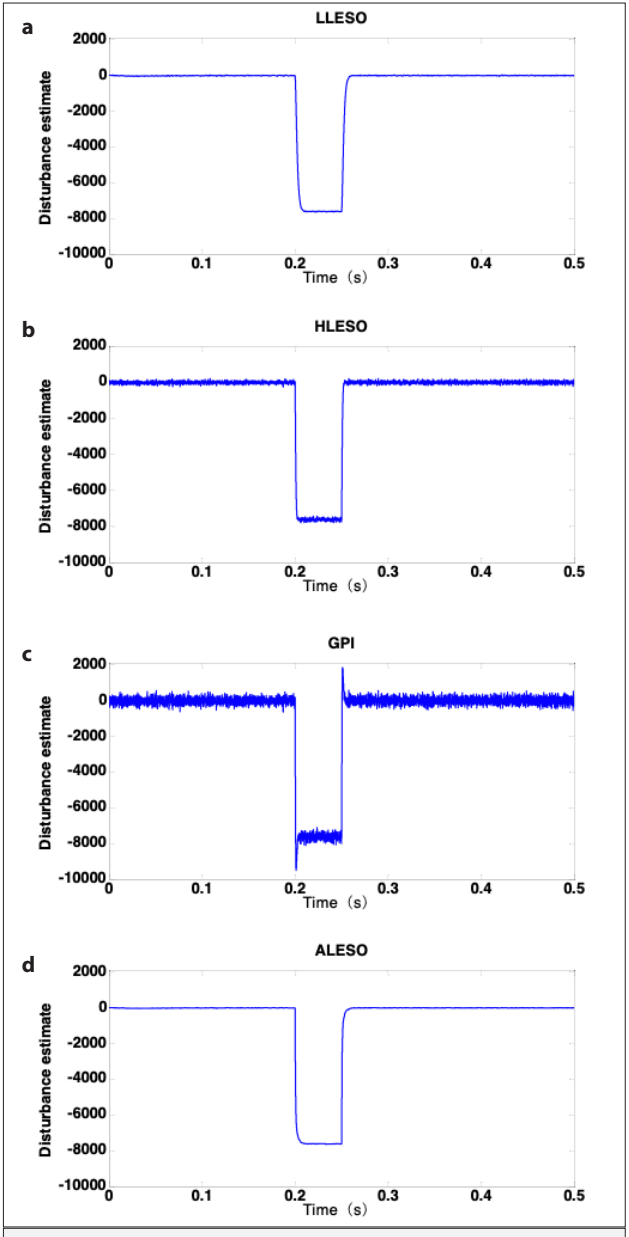

Figure 13. a-d. The disturbance estimation $\hat{f}$ of four disturbance observers: (a) LLESO, (b) HLESO, (c) GPI observer, and (d) ALESO

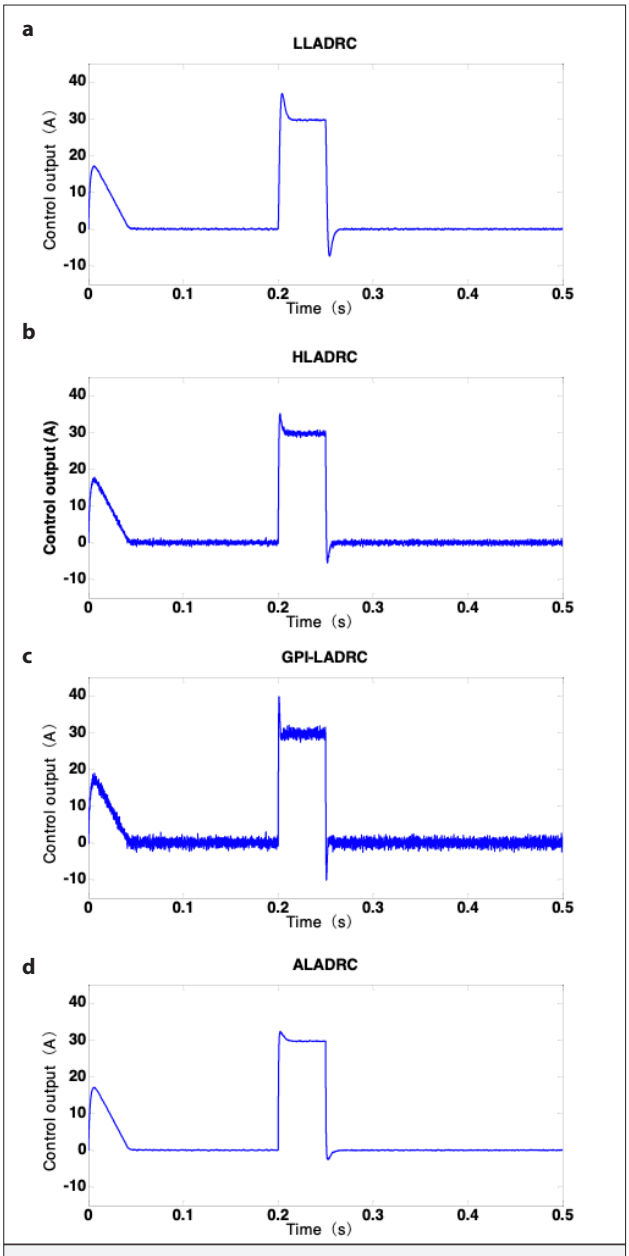

Figure 14. a-d. The control output i_q^* of four speed control methods: (a) LLADRC, (b) HLADRC, (c) GPI-LADRC, and (d) ALADRC

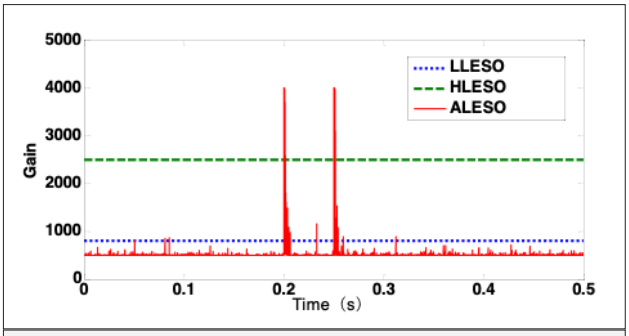

Figure 15. The observation gain of ALESO

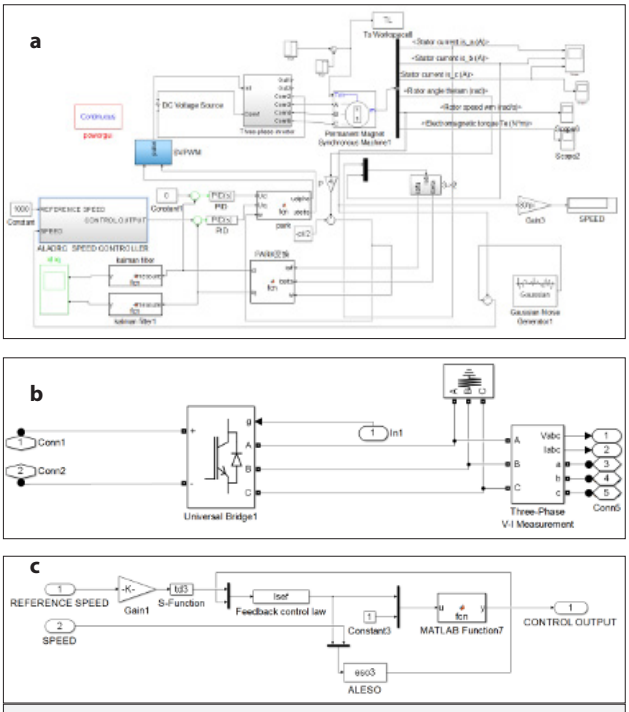

Figure 16. a-c. SIMULINK simulation model of PMSM ALADRC speed control system: (a) the main system, (b) the subsystem of ALADRC speed controller, (c) the subsystem of Three-phase inverter

T_L=30, the IMASE of ALADRC and LLADRC is far smaller than that of HLADRC and GPI-LADRC. It can be seen that LLADRC and ALADRC have much higher steady speed control accuracy than HLADRC and GPI-LADRC. Figures 13 and 14 and Table 6 give the reason. The steady speed control accuracy of the system is positively correlated with the noise suppression ability of the system. It can be seen from Table 6 that in the case of containing measurement noise, the IMADE of ALESO and LLESO is much smaller than that of HLESO and GPI observer, which means that the steady-state accuracy of disturbance tracking of the former two is higher, which can also be directly verified from Figure 13. By comparing Figure 6 with Figure 13, the disturbance estimation values of HLESO and GPI observers are highly polluted by noise in steady state, while LLESO and ALESO are almost unaffected. As the control quantity i_q^* is directly compensated by the disturbance estimation value, the noise from HLESO and

Table 6. The IMADE of the four disturbance observer

Disturbance Observer	IMADE	
	T_L=0	T_L=30
LLESO	8.521	8.6454
HLESO	48.683	43.782
GPI	128.399	116.4169
ALESO	4.4325	6.8581

Table 7. The IMASE of the four control methods

Control method	IMASE	
	T_L=0	T_L=30
LLADRC	0.159	0.1505
HLADRC	0.2325	0.2254
GPI-ADRC	0.362	0.3174
ALADRC	0.139	0.1841

GPI observers is directly introduced into i_q^*, which can be seen directly from Figure 14. This will undoubtedly affect the speed control accuracy of the system.

According to Table 6, the IMADE of ALESO is the smallest regardless of T_L=0 or T_L=30. This means that ALESO has the optimal steady-state tracking accuracy and noise suppression capability. This is due to the small gain of ALESO in steady state, which can be seen directly from Figure 15. Due to the existence of the low gain stationary region of the gain adaptive law, $\xi(|e_1|)$ is less sensitive to noise in the steady state, and the gain of ALESO is smaller than that of LLESO in most of the time. Therefore, ALESO is even stronger than LLESO in suppressing noise.

In practical engineering applications, the width of the low-gain stationary region of $\xi(|e_1|)$ can be planned according to the amplitude of the noise, and then the width of the low-gain stationary region can be adjusted by adjusting the size of μ and δ, so that the noise performance of ALESO can be optimized.

Conclusion

In this paper, a gain adaptive linear extended state observer (ALESO) based active disturbance rejection speed controller (ALADRC) of PMSM vector control system is proposed and the gain adaptive law of ALESO is designed. The error convergence of ALESO is analyzed and the boundedness of the tracking error is proved. Finally, the performance of ALADRC speed controller is verified by simulation, and it is concluded that, compared with LLADRC for poor load resistance and robustness, and HLADRC and GPI-LADRC for serious noise pollution, ALADRC has excellent anti-interference ability and noise suppression ability.

Appendix

Proof of Theorem 1

The proof requires citing the facts [17] is as follows

Fact: From (8), it is observed that if e_1 identically zero, then $e_2 = 0$. If e_1 is not identically zero, but ultimately uniformly arbitrarily close to zero, then $z_{22}= \hat{f}$ would also be an ultimately arbitrarily close estimate of f. Similarly, if e_1 is bounded, then e_2 is bounded as well.

The gain adaptive law $\xi(|e_1|)$ as show in Figure 3 can be divided into high-gain linear region and nonlinear region.Defining that σ is a constant determined by the width of the nonlinear region of $\xi(|e_1|)$.

The first step: The error convergence of linear extended state observer is analyzed as follows.

Assume that the observation gain of the linear extended state observer of (5) is $\overline{w}_0$, and its differential equation of state error is similar to (8), which can be written in the following standard form.

$$\dot{e} = A_0 e + \eta \tag{21}$$

where

$$e = [e_1 \;\; e_2]^T = [z_{21} - w \;\; z_{22} - f]^T, A_0 = \begin{bmatrix} -2\overline{w}_0 & 1 \\ -\overline{w}_0{}^2 & 0 \end{bmatrix}, \eta = \begin{bmatrix} 0 \\ \dot{f} \end{bmatrix} \tag{22}$$

For (21), consider the following Lyapunov function

$$V = e^T P_0 e \tag{23}$$

If $w_0 > 0$, then A_0 is Hurwitz, then there must be a positive definite matrix P_0 that satisfies this Riccati equation $A_0^T P_0 + P_0 A_0 = -I$.

Calculate the derivative of V along the solution of (21) as follows,

$$\begin{aligned} \dot{V}(e) &= e^T \left(A_0^T P_0 + P_0 A_0\right) e + \eta^T P_0 e + e^T P_0 \eta \\ &\le -\|e\|^2 + 2\|e\| \cdot \|\eta\| \cdot \|P_0\| \\ &\le -\|e\|(\|e\| - 2\gamma \|P_0\|) \end{aligned} \tag{24}$$

Then, when $\|e\| \ge 2\gamma\|P_0\|$, $\dot{V}(e) \le 0$. So there must be $t_0 > 0$, which can lead to $\|e\| \le 2\gamma\|P_0\|, \forall t \ge t_0$

The second step: The tracking error convergence of ALESO is analyzed as follows.

It can be known from the properties of $\xi(|e_1|)$ and Figure 3, when e_1 is in the high-gain linear region, that is, $e_1 \in (-\infty, -e_n) \cup (e_n, +\infty)$, $\xi(|e_1|)$ hardly changes with e_1, and it can be considered that

$$\xi(|e_1|) = B + 0.5a, e \in (-\infty, -e_n) \cup (e_n, +\infty) \tag{25}$$

At this point, ALESO can be considered as LESO with constant observed gain $\overline{w} = B + 0.5a$.

The initial error $e_1(0)$ of e_1 is divided into the following two cases.

Case 1: $e_1(0) \in (-e_n, e_n)$

Case 2: $e_1(0) \in (-\infty, -e_n) \cup (e_n, +\infty)$

Error convergence analysis of ALESO in case 1:

When $e_1(0) \in (-e_n, e_n)$, there are two possible development trends in e_1 of ALESO.

Possible development trend 1:

e_1 is always in the nonlinear interval ($-e_n$, e_n), where e_1 is bounded as

$$|e_1| \le e_n \tag{26}$$

According to fact, e_2 is eventually bounded and then

$$||e|| \le \sigma \tag{27}$$

where σ is determined by e_n.

Possible development trend 2:

e_1 moves to interval $(-\infty, -e_n)$ or interval $(e_n, +\infty)$, then at this point, ALESO is linear and the gain of ALESO is constant

$$\overline{w} = \xi_{\max}(|e_1|) = B + 0.5a$$

Thus, according to the analysis of the error convergence of LESO, there must be $t_1 > 0$, which can lead to

$$\|e\| \le 2\gamma\|P_1\|, \forall t \ge t_1 \tag{28}$$

where P_1 is the solution of Riccati equation of

$$A_1^T P_1 + P_1 A_1 = -I, A_1 = \begin{bmatrix} -2(B+2a) & 1 \\ -(B+2a)^2 & 0 \end{bmatrix}$$

Error convergence analysis of ALESO in case 2:

When, $e_1(0) \in (-\infty, -e_n) \cup (e_n, +\infty)$ there are two possible development trends in e_1 of ALESO.

Possible development trend 1:

e_1 is always in the linear interval $(-\infty, -e_n) \cup (e_n, +\infty)$

Possible development trend 2:

When e_1 moves to nonlinear interval ($-e_n$, e_n), for either trend 1 or trend 2 in case 2, both the derivation and the final result is the same as case 1.

Combining the above, for either case 1 or case 2, the tracking error, e, are ultimately bounded as

$$\|e\| \le \max(2\gamma\|P_1\|, \sigma)$$

If $\xi_{\max}(|e_1|)$ is large enough, then e_1 must develop to the nonlinear interval and eventually be constrained to interval ($-e_n$, e_n).

e is eventually bounded as (27). The narrower the nonlinear interval of $\xi(|e_1|)$, the smaller σ, and the higher the observation accuracy of ALESO.

Otherwise e is bounded as (28). Therefore, the upper limit and the width of the nonlinear interval of $\xi(|e_1|)$ jointly determine the tracking accuracy of ALESO.

Further, if $\dot{f}$ ultimately being equal to zero, that is,

$$d = \dot{f} = 0 \tag{29}$$

According to (8) and (29), the solution of (8), e would ultimately reaches very close to zero.

Peer-review: Externally peer-reviewed.

Conflict of Interest: The authors have no conflicts of interest to declare.

Financial Disclosure: The authors declared that the study has received no financial support.

References

1. H. H. Choi, N. T. Vu, J. Jung, "Digital Implementation of an Adaptive Speed Regulator for a PMSM", IEEE Transactions on Power Electronics, vol. 26, no. 1, pp. 3-8, Jan. 2011. [CrossRef]
2. Y. A.-R. I. Mohamed, "A hybrid-type variable-structure instantaneous torque control with a robust adaptive torque observer for a high-performance direct-drive PMSM", IEEE Trans. Ind. Electron, vol. 54, no. 5, pp. 2491-2499, Oct. 2007. [CrossRef]
3. D. Seo, Y. Bak, S. Cho, K. Bae, K. Lee, "An Improved Flying Restart Method of Sensorless PMSM Drive Systems Fed by an ANPC Inverter Using Repetitive Zero Voltage Vectors", in 2019 IEEE Applied Power Electronics Conference and Exposition (APEC), Anaheim, CA, USA, 2019, pp. 3309-3314. [CrossRef]
4. M. Konghirun, L. Xu, "A Fast Transient-Current Control Strategy in Sensorless Vector-Controlled Permanent Magnet Synchronous Motor", IEEE Transactions on Power Electronics, vol. 21, no. 5, pp. 1508-1512, Sept. 2006. [CrossRef]
5. B. Bıdıklı, "A Self-Tuning PID Control Method for Multi-Input-Multi-Output Nonlinear Systems", Electrica, vol. 18, no. 2, pp. 218-226, 2018. [CrossRef]
6. G. Zhang, G. Wang, B. Yuan, R. Liu, D. Xu, "Active Disturbance Rejection Control Strategy for Signal Injection-Based Sensorless IPMSM Drives", IEEE Transactions on Transportation Electrification, vol. 4, no. 1, pp. 330-339, March 2018. [CrossRef]
7. Y. Taskin, "FUZZY PID CONTROLLER FOR PROPELLER PENDULUM", IU-Journal of Electrical & Electronics Engineering, vol. 17, no. 1, pp. 3201-3207, 2017.
8. S. Li, H. Gu, "Fuzzy Adaptive Internal Model Control Schemes for PMSM Speed-Regulation System", IEEE Transactions on Industrial Informatics, vol. 8, no. 4, pp. 767-779, Nov. 2012. [CrossRef]
9. G. Zhiqiang, "Scaling and bandwidth-parameterization based controller tuning", in Proceedings of the 2003 American Control Conference, 2003., Denver, CO, USA, 2003, pp. 4989-4996.
10. G. Liu, L. Q. Jin, "Stability Control System of Distributed Drive Electric Vehicles Using Linear Active Disturbance-Rejection Control", Journal of Beijing Institute of Technology, vol. 37, no. 3, pp. 250-254, 2017.
11. Z. Q. Chen, M. V. Sun, R. G. Yang, "On the Stability of Linear Active Disturbance Rejection Contro", ACTA AUTOMATICA SINICA, vol. 39, no. 5, pp. 574-580, 2014. [CrossRef]
12. S. Qiusheng, Z. Yuejin, "Improvement of linear expansion state observer and analysis of observation accuracy", Journal of national university of defense technology, vol. 39, no. 06, pp. 111-117, 2017.
13. Y. X. Su C. H. Zheng, B. Y. Duan, "Automatic disturbances rejection controller for precise motion control of permanent-magnet synchronous motors", IEEE Trans. Ind. Electron, vol. 52, no. 3, pp. 814-823, Jun. 2005. [CrossRef]
14. B. Du S. Wu S. Han S. Cui, "Application of linear active disturbance rejection controller for sensorless control of internal permanent-magnet synchronous motor", IEEE Trans. Ind. Electron, vol. 63, no. 5, pp. 3019-3027, May 2016. [CrossRef]
15. J. Wen, B. Cao, "Active disturbances rejection control speed control system for sensorless IPMSM", in Zhongguo Dianji Gongcheng Xuebao/Proc. CSEE., vol. 29, no. 30, pp. 58-62, Oct. 2009.
16. Y. Dong, M. Xiaojun, Z. Qinghan, Q. Xiaobo, "Study on frequency band characteristics and parameter configuration of LADRC for second-order systems", Control theory and application, vol. 30, no. 12, pp. 1630-1640, 2013.
17. H. Sira-Ramírez, J. Linares-Flores, C. García-Rodríguez, M. A. Contreras-Ordaz, "On the Control of the Permanent Magnet Synchronous Motor: An Active Disturbance Rejection Control Approach", IEEE Transactions on Control Systems Technology, vol. 22, no. 5, pp. 2056-2063, Sept. 2014. [CrossRef]
18. L. Fei, S. Hu, Z. Qionglin, X. Yanfeng, "A new type of extended state observer with measurement noise", Control theory and application, vol. 06, pp. 995-998, Dec. 2005.
19. Z. Pu, R. Yuan, J. Yi, X. Tan, "A Class of Adaptive Extended State Observers for Nonlinear Disturbed Systems", IEEE Transactions on Industrial Electronics, vol. 62, no. 9, pp. 5858-5869, Sept. 2015. [CrossRef]

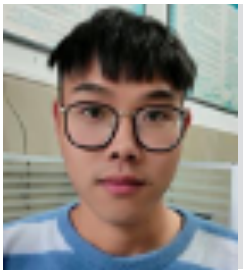

Yinsheng Li received his bachelor's degree in engineering from Wuyi university, Guangdong province,China in 2018.He is currently studying for a master's degree at Yangtze university,hubei province,China.His main research interests include:electronics and electrical transmission,active disturbance control and robust control.

Yongjun Chen is associate dean, professor, PhD, and master tutor of school of electronic information, Yangtze University. He is a senior visiting scholar at aalborg university in Denmark, where his research interests include power electronics and electrical drives and control of special motors.